Nuclear Engineering and Design 409 (2023) 112349

Contents lists available at ScienceDirect

Nuclear Engineering and Design

journal homepage: www.elsevier.com/locate/nucengdes

Numerical analyses of the CIRCE-THETIS facility by mean of STH and CFD codes

Pietro Stefanini [a,*], Andrea Pucciarelli [a], Nicola Forgione [a], Ivan Di Piazza [b], Daniele Martelli [b]

[a] Università di Pisa, Dipartimento di Ingegneria Civile e Industriale, Largo Lucio Lazzarino 2, 56122 Pisa, Italy
[b] ENEA Brasimone R.C, Camugnano, Italy

A B S T R A C T

During the last decade the European Union funded numerous projects with the aim to pave the way for the development of Gen IV nuclear reactor technologies. The recently started EU project PATRICIA, to which the University of Pisa participates, provides room for further investigations of the involved phenomena in LMFRs (e.g. thermal stratification inside the pool, LBE heat transfer capabilities, transition from forced to natural circulation) by means of both experimental and numerical analyses. In the frame of the PATRICIA project, the ENEA Brasimone Research Centre foresees to carry-out an experimental campaign involving the CIRCE facility. With respect to the previous configurations, the facility will be updated substituting the steam generator, which will exhibit an helicoidal steam generator (THETIS): the experimental campaign will involve the analysis of steady-state and postulated accidental scenarios. The University of Pisa provides numerical support both in the pre-test and post-test phases to assist the design of the experiment. This work reports about the preliminary results obtained by numerical simulations of the CIRCE-THETIS facility. The analyses were performed both using CFD codes (ANSYS Fluent) and STH codes (RELAP5-3D). The analyses mainly focused on temperature and velocity distributions inside the CIRCE pool during the postulated nominal steady-state conditions. In addition, a transient analysis was performed investigating the behaviour of the addressed facility in case of a PLOFA scenario. The limits and capabilities of both the approaches were observed and are discussed in the present work trying to provide guidelines for a correct application of the adopted codes. The obtained results provide interesting suggestions for the experimentalists and represent a valuable support in better setting the experimental conditions and measurements tools layout.

1. Introduction

Obtaining a good representation of the phenomena involved in liquid metals thermal-hydraulics (e.g. thermal stratification inside the pool, LBE heat transfer capabilities, transition from forced to natural circulation) still represents one of the key issues to be solved for the development of the upcoming GEN IV Liquid Metal Fast Reactors (LMFRs). Liquid Metals (LM) represent a further step in terms of safety and efficiency (IRSN, 2012; Nuclear Energy Agency, 2015) for new nuclear power reactors. From a neutronic point of view LM present a low moderation capability: this allows to exploit a fast neutron spectrum, enabling for burning long-lived fission products and for breeding reactions. On the other hand, their large heat capacity and heat transfer capabilities make them a very interesting coolant for the primary system. For these reasons, in the last decade many EU projects aimed to develop this technology by means of both experimental and numerical analyses (e.g. PATRICIA (PATRICIA, 2020), MYRTE (MYRTE Project, 2015) and SESAME (SESAME, 2020). Among the main purposes of these projects there were the analysis of heat transfer capabilities of liquid metals and the investigation of the chance of adopting passive decay heat removal systems. Several experimental facilities were established in order to support the common effort, e.g. TALL-3D (Grishchenko et al., 2015), E-SCAPE (Van Tichelen and Mirelli, 2017) and CIRCE (Lorusso et al., 2021).

In the frame of the ongoing EU PATRICIA (PATRICIA, 2020) project, the ENEA Brasimone Research Centre foresees to carry-out an experimental campaign involving a new configuration for the CIRCE facility: a new steam generator with an innovative helical coil design, named THETIS, will be installed inside the already existing CIRCE-pool (Lorusso et al., 2021). Further modifications will be applied to the loop side: forced circulation will no more be achieved through the Argon injection system, which will be substituted by a Main Coolant Pump (MCP).

In the present paper, the thermal–hydraulic analysis of the new CIRCE-THETIS configuration is performed. The analysis was carried on by means of STH and CFD codes: in particular, RELAP5-3D was used as STH code (RELAP5-3D Code Manual, 2018) and ANSYS Fluent (ANSYS, Inc.) was adopted for what concerns the CFD part. The two codes were also considered in previous analyses which provided a preliminary validation of the modelling tools. This process of validation was performed by simulating the old CIRCE-HERO configuration (Pesetti et al., 2018) with the two codes and comparing the obtained results with the

* Corresponding author.
E-mail addresses: p.stefanini@studenti.unipi.it (P. Stefanini), andrea.pucciarelli@unipi.it (A. Pucciarelli), nicola.forgione@unipi.it (N. Forgione), ivan.dipiazza@enea.it (I. Di Piazza), daniele.martelli@enea.it (D. Martelli).

https://doi.org/10.1016/j.nucengdes.2023.112349
Received 30 January 2023; Received in revised form 20 April 2023; Accepted 20 April 2023
Available online 27 April 2023

Nomenclature

CFD	Computational Fluid Dynamics
CIRCE	CIRColazione Eutettico
E-SCAPE	European SCaled Pool Experiment
FPS	Fuel Pin Simulator
FV	Fitting Volume
HCSG	Helical Coil Steam Generator
HERO	Heavy liquid mEtal pRessurized water cOoled tubes
HX	Heat eXchanger
LBE	Led Bismuth Eutectic
LM	Liquid Metal
LMFRs	Liquid Metal Fast Reactors
MCP	Main Coolant Pump
MYRTE	MYRRHA Research and Transmutation Endeavour
PATRICIA	Partitioning and Trasmuting Research Initiative in a Collaborative Innovation Action
PLOFA	Protected loss of flow accident
SESAME	Thermal hydraulic Simulations and Experiments for the Safety Assesment of MEtal cooled reactors
SG	Steam generator
STH	System Thermal Hydraulic
TALL-3D	Therml hydrAulics LBE Loop with 3D test section
THETIS	Thermal-hydraulic HElical Tubes Innovative System
TMDPV	Time dependent volume

available experimental data (Lorusso et al., 2018). In the past works, attention was mainly paid to the assessment of the capabilities of the considered codes in reproducing the thermal stratification phenomena occurring inside the pool (Buzzi et al., 2020; Moscardini et al., 2020; Stefanini, 2021; Buzzi et al., 2020); mesh validation and sensitivity analyses were performed as well (Stefanini, 2021). The obtained results were promising and both steady-state and transient conditions were simulated with a sufficient accuracy. In particular, the CFD codes allowed for the prediction of the thermal stratification occurring in the pool during the experimental campaign: good predictions for this phenomenon were provided by STH codes, too (Stefanini et al., 2023; Stefanini et al., 2022). Experimental transient conditions were successfully reproduced by means of RELAP5/Mod3.3 for both the primary and secondary side. Coupled STH/CFD calculations were performed as well for some selected transient conditions, showing nice improvements with respect to both the stand-alone applications (Galleni et al., 2020). As a consequence, both due to the performed validation process on the modelling tools (also validated against other experimental campaigns involving the NACIE-UP facility, see e.g. (Pucciarelli et al., December 2020)and to the similar phenomena expected to occur in the new CIRCE-THETIS configuration, the adopted modelling techniques should allow for suitable pre-test analyses in support of the upcoming experimental campaign.

Two reference cases for the CIRCE-THETIS facility were thus considered in the frame of the present work (di Piazza et al., 2020) in support of the upcoming experimental campaign: a steady-state case, considering the foreseen nominal operating conditions, and a possible transient scenario. In the RELAP5-3D application the CIRCE-pool was simulated as a 3D component while the other loop components were kept mono dimensional. For this code, a closed loop was considered in order to investigate the postulated transients. For the CFD, instead, an open loop was considered and, for the transient, only the final steady state conditions were simulated, in similarity with the analysed performed in the frame of the CIRCE-HERO campaign carried on during the MYRTE project. Being pre-test analyses, the boundary conditions for the final steady state for the CFD simulation were provided via precursor calculations performed using RELAP5-3D: the STH results were in fact used as a basis for the definition of the boundary conditions for the CFD simulation.

The performed analyses report interesting results highlighting both capabilities and potential flaws of the adopted numerical models, providing valuable suggestions for both numerical and experimental people. The lessons drawn will be later considered to prepare more detailed modelling tools for both stand-alone and coupled STH/CFD calculations that should allow for improved predictions of the upcoming experimental results.

2. Facility description and considered experimental conditions

CIRCE is an integral effects test facility made of AISI 316L stainless steel designed to hold about 70 tons of Lead-Bismuth Eutectic alloy (LBE); the pool includes a primary circuit that allows for natural and forced circulation of the LBE. The primary loop consists of the Feeding Conduit (FC), the Fuel Pins Simulator (FPS), the Fitting Volume (FV), the Main Coolant Pump (MCP), the Riser, the Separator, and the new

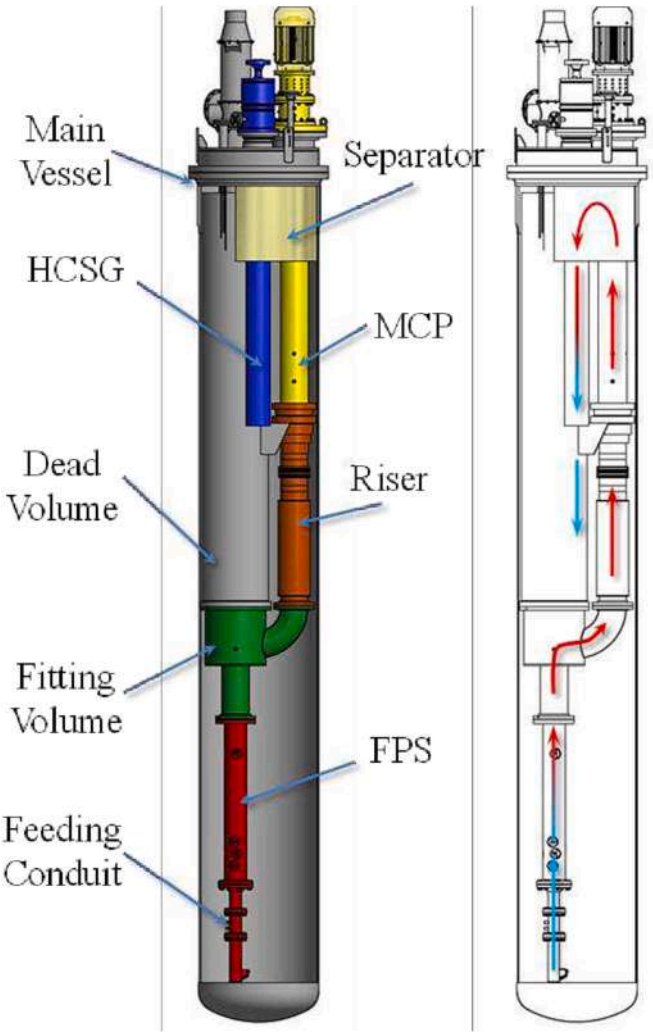

Fig. 1. Full view of the flow path and the main component of CIRCE-THETIS facility, taken from (Lorusso et al., 2021).

HeliCoidal Steam Generator (HCSG) (Lorusso et al., 2021). Fig. 1 shows the flow path of the LBE inside the loop: LBE enters in the FPS region from the Feeding conduit; here it is heated up by the electrical heaters of the FPS. Once it reaches the top part of the FPS, the LBE enters inside the FV where it is collected and directed towards the Riser, the MCP and the Separator. After the Separator, LBE flows downward inside the steam generator, where it is cooled down by water and steam flowing inside the helical pipes.

The secondary side is composed of a once-through loop where pressurized water at 18 MPa enters inside the loop and superheated steams exits. The THETIS steam generator consists of an outer shell where LBE flows and 15 helical pipes arranged in three ranks, where water and steam flow. The pipes active length is about 6 m and, based on a design evaluation, THETIS is foreseen to be able to exchange about 450 kW_{th} in the planned operating conditions.

In the present paper the reference steady state conditions and a postulated transient scenario were considered for the numerical analyses. The operating condition suggested by ENEA (di Piazza et al., 2020), resumed in the Table 1 and Table 2, were considered as reference.

3. Adopted nodalization and mesh setting

3.1. RELAP5-3D nodalization

The STH code RELAP5-3D was used for the performed analyses. With respect to the RELAP5/Mod3.3 adopted in previous works (Moscardini et al., 2020), this code allows the user to simulate 3D components. In the present analysis, only the pool was represented by a 3D pipe, while the internal loop was modelled using 1D thermal-hydraulics components. The main aim of this choice is to achieve an improved analysis of the pool region, while acting in similarity with the past RELAP5/Mod3.3 applications for the loop components, for which suitable results were already achieved in past experiences. The pool was thus represented as a 3D pipe having 6 azimuthal subdivisions 4 radial subdivisions and 50 axial subdivisions, trying to follow the actual geometry of the experimental facility. Inside the pool, volume factors were considered taking in account the volume occupied by the internal loop elements. Fig. 2, shows the most relevant pool sections: the volume factors were calculated in accordance with the percentage of horizontal surface of each sector (i.e. the blue light regions) not occupied by the internal loop components (i.e. the circles in the proposed figure). It must be stressed that for the new geometry of the HCSG THETIS, no heat transfer correlations for helical tubes are implemented inside the code; this aspect is to be better investigated in the frame of future works, which will also consider the chance to implement heat transfer specific correlations for the addressed geometry. A scheme of the nodalization adopted for the steam generator tubes is shown in Fig. 3. The new HCSG was here represented as an annulus component for the LBE side, while the helical pipes, where water and steam flow, were represented as a single inclined pipe having the same flow area and the active length of the 15 tubes. The elevation of the pipe was set equal to the real elevation of the steam generator being 1.5 m. This type of scheme is widely used in literature (Lian et al., 2020; Xu et al., 2021).

Aiming to represent the postulated transient, a closed loop was simulated. A scheme of the loop is reported in Fig. 4. It must be stressed out that in RELAP5-3D, no axial heat conduction, neither azimuthal nor radial, are present: this implies that the heating up of the pool occurs only thanks to e convection. The hotter fluid is collected in the upper region due to buoyancies forces and it is almost thermally insulated from the colder fluid in the bottom part. This may also imply problems when heat transfer towards the environment is considered: the colder region at the bottom of the pool would thus be cooled down until it reaches the room temperature, resulting in a nonphysical meaning. For this reason, no heat exchange towards the environment is assumed at the pool external boundaries for this preliminary analyses. This contribution will instead be considered in future works in order to better comply with the actual experimental conditions. As a further remark, the ongoing analyses seem supporting the results reported in the present paper, thus suggesting that at least the main phenomena were already sufficiently well captured even with the presently considered assumptions.

In addition, it must be highlighted that some simplifying assumptions were considered for the cover gas region. During the preliminary tests, the connection between the 3D component hosting the cover gas and the time dependent volume led to stability issues due to the gas–liquid interface. The problem was later solved introducing a 1D branch component in between, which let the liquid/gas interface be positioned in a 1D environment, thus making the numerical problem easier and avoiding stability problems. Nevertheless, very small time-steps were required, thus implying an unnecessary long computational time. The results of this configuration were compared with the ones provided by a model neglecting the cover gas region (the one in Fig. 4). Since no relevant changes were observed, except for the far smaller computational time of the latter one, the model neglecting the cover gas region was considered for this preliminary application.

Fig. 5 reports the scheme of the component depicted in green in Fig. 4. It is a switching mechanism composed by two motor valves, a time dependent junction and a single junction which aims at simulating the MCP. This tool was introduced to allow the transition between forced circulation, provided by the MCP, and the natural circulation occurring once that the MCP is completely switched off during the initial seconds of the postulated transient. The time dependent junction was preferred to the pump component owing its easier deployment. Setting up a suitable pump component, needs a very good estimation of several parameters (the loop pressure drops, the characteristic curve, rpms…): this tuning process seemed to require too many efforts for the addressed preliminary calculations. The adopted switching mechanism was thus introduced allowing for a more direct setting of the mass flow rate through the time-dependent junction while providing room for the natural circulation. A pump component will be considered in future studies, once all the characteristics of the pool and loop environment will be defined by the final design.

3.2. CFD mesh setting

CFD simulations were performed adopting ANSYS Fluent because of the good experience gained at the University of Pisa in the frame of previous works (see e.g. (Buzzi et al., 2020; Stefanini, 2021; Buzzi et al., 2020) and since it represents one of the cornerstones of the coupled STH/CFD methodology developed at UniPi (Pucciarelli et al., 2020, 2021). The present work also focuses on the prediction of possible

Table 1
Nominal steady state boundary conditions.

Reference case	unit	Value
$T_{in-\ pool}$	°C	400
FPS power	kW	450
Mass flow rate LBE	kg/s	35.17
Mass flow rate H_2O	kg/s	0.26
Pressure H_2O	bar	180
$T_{in\text{-}h2o}$	°C	335

Table 2
Postulated transient.

Transient	Time starts	Time end	Final value
Scram	0 s	240 s	5%*
Feed water reduction	0 s	3 s	10%**
MCP reduction	1 s	11 s	0%**

*The reduction follows a postulated decay heat curve.
**A linear reduction is assumed.

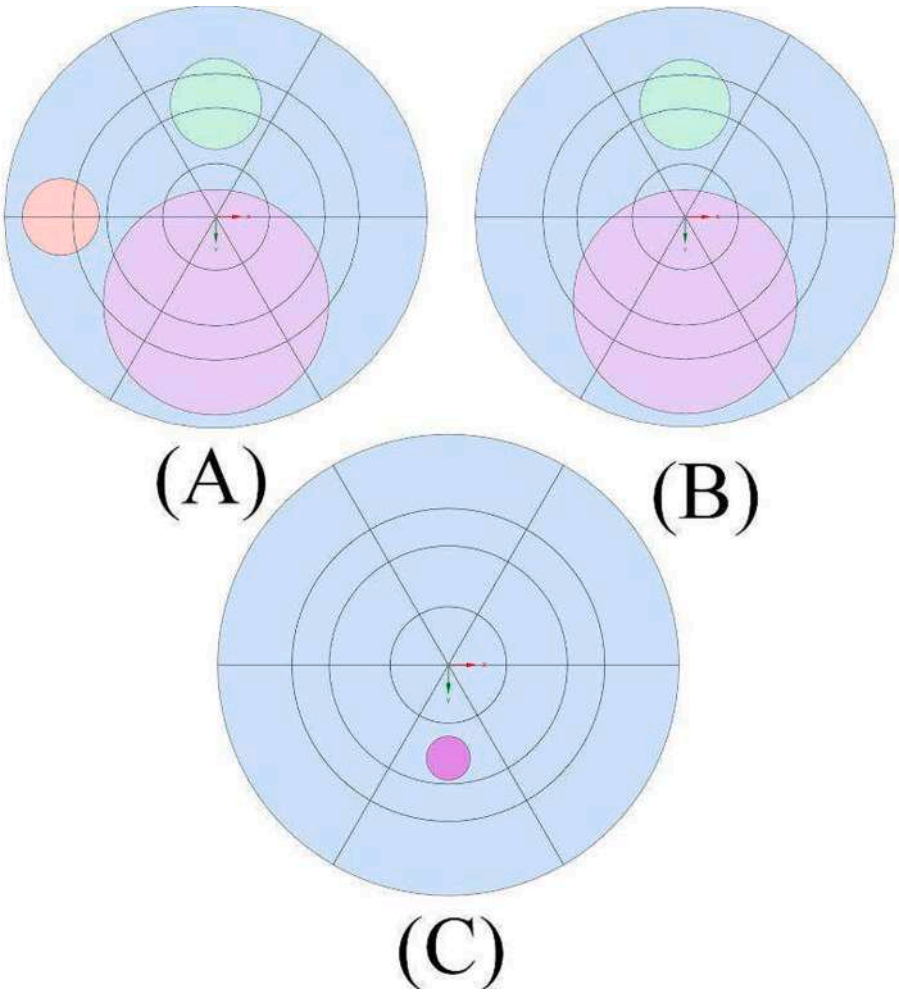

Fig. 2. Scheme showing the strategy adopted for the calculation of the volume factor inside the 3D pool: (A) section above the HSCG outlet; (B) section below the HCSG outlet; (C) bottom section.

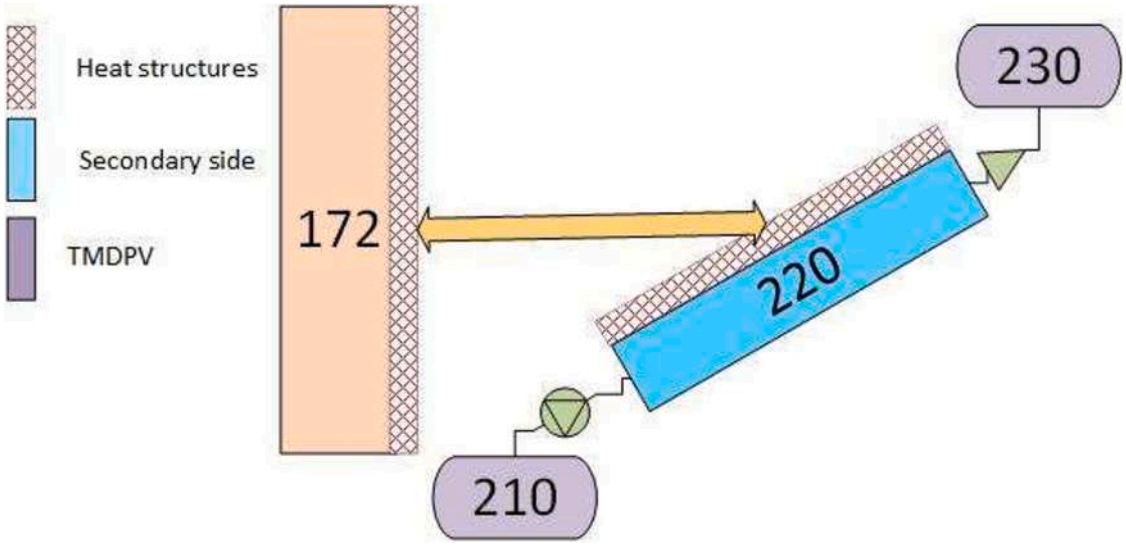

Fig. 3. Adopted nodalization for the HCSG.

thermal distributions occurring inside the CIRCE pool. In the present work, in order to reduce the computational costs, the CFD domain only consists of the pool region, thus excluding the internal components of the loop and the external wall of the vessel. It must be stressed that, for this CFD application, the reference nominal steady state conditions were simulated, while for the postulated transient only the final steady state

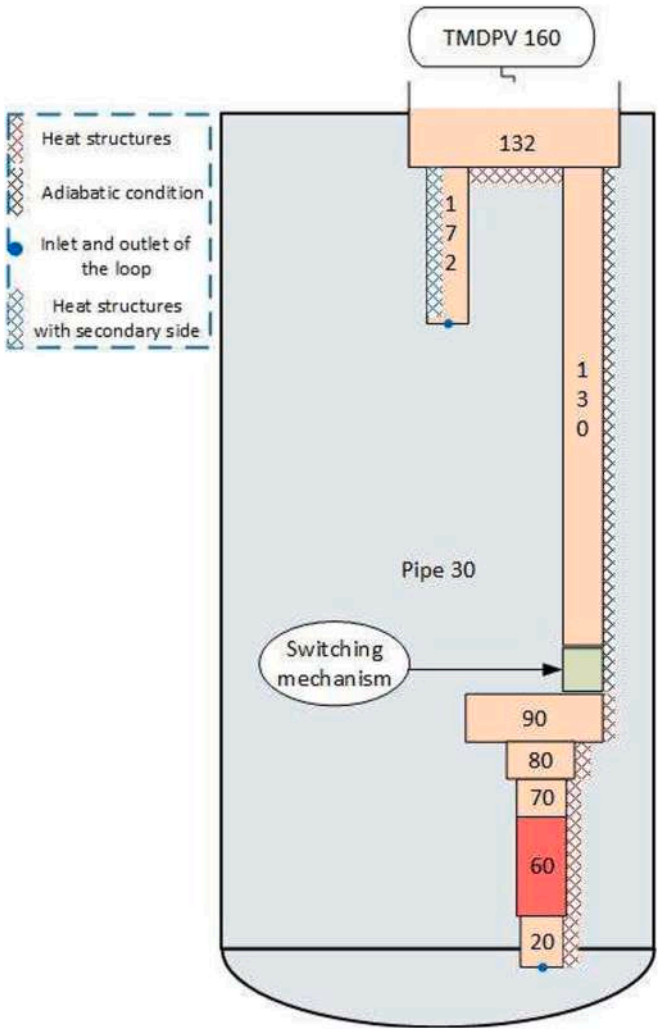

Fig. 4. Closed loop representation: the Switching Mechanism (S.M.) is reported in green.

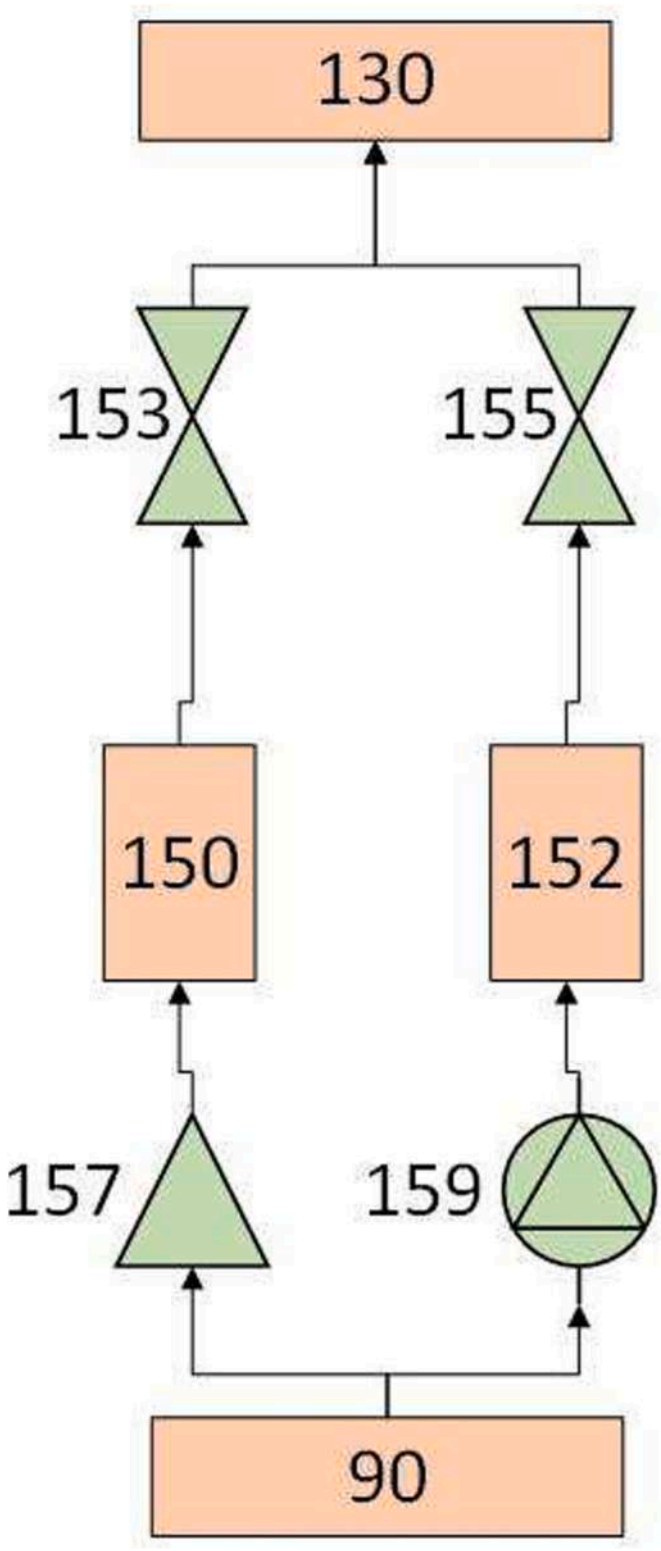

Fig. 5. Switching mechanism nodalization.

was considered deriving the corresponding boundary conditions from the STH simulation, in which the entire transient was instead simulated.

Fig. 6 shows the boundary conditions applied to the CFD domain: an imposed mass flow rate, equal to the one to be considered in the nominal conditions (di Piazza et al., 2020) for the steady state case, was set at the THETIS outlet. For the final steady-state occurring after the transient, instead, this value was set in accordance with the one predicted by RELAP5-3D. The heat exchange trough the FPS and FV walls was simulated through a convective heat transfer condition. It must be stressed that, being pre-test analyses, the wall temperature profile imposed on the heated region was set in accordance with the STH predictions as well. In this sense, data from RELAP5-3D were used as a precursor simulation for ANSYS Fluent. A convective heat transfer coefficient of 3500 W/m^2K was derived by calculating the equivalent resistance between the internal loop and the pool environment. Eventually, heat transfer towards the environment was also included in the model: a heat transfer coefficient of 2.5 W/m^2K and a room temperature of 298.15 K were taken as reference, in accordance with previous works on the same facility (Pucciarelli et al.). For what concerns the adopted mesh, the settings were selected in accordance with previous works performed at the University of Pisa (Buzzi et al., 2020; Stefanini, 2021; Buzzi et al., 2020), thus guaranteeing the suitability of the obtained mesh. Following other works in this field, calculations were performed adopting the SST-k-ω turbulence model, which seems to be among the most reliable ones for this kind of applications; a turbulent Prandtl number of 1.5 was also assumed, in accordance with the vast majority of the works proposed in the available literature (see e.g. (Buzzi et al., 2020; Pucciarelli et al., 2020, 2021; Stefanini, 2021; Stefanini et al., 2023; Zwijsen et al., 2019; Buzzi et al., 2020; Nuclear Energy Agency, 2015). Fig. 7 shows the obtained nodalization for three selected sections of the pool while Table 3 resumes the main settings considered for the generation of the mesh. Though the considered assumptions may look

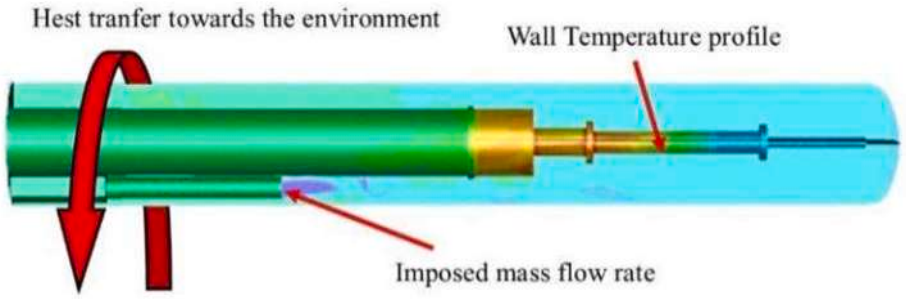

Fig. 6. Boundary conditions for THETIS.

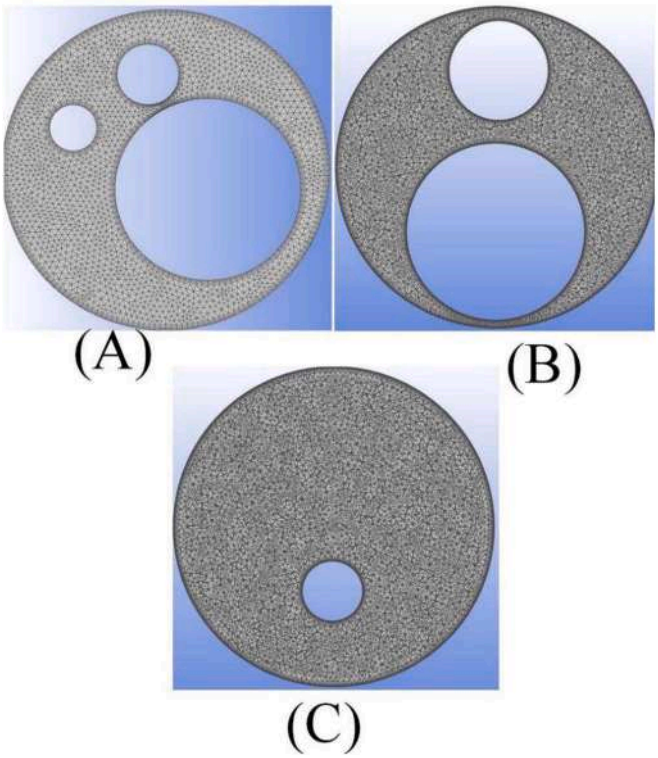

Fig. 7. Sections representative of the obtained mesh for the pool environment: (A) above THETIS outlet section; (B) below THETIS outlet section; (C) bottom section.

Table 3
CFD Mesh Setting.

Fluent setting	Value
Element Size	0.02 m
Capture proximity	0.001
Prism stretching	1.5
Number of layers	10
Prism thickness	0.02 m
Total number of cells	16,607,353

relevant, the ongoing calculations considering a domain simulating the whole facility (pool, loop, structures …) supports the results provided hereinafter, thus suggesting, again, that the main phenomena were already sufficiently well captured even with the presently considered assumptions.

4. Results

4.1. Test reference – nominal steady state

The present section reports the results provided for the considered steady-state case by the two selected codes. Fig. 8 shows the comparison between the temperature distribution predicted inside the pool by the two codes. As it can be observed, the two codes predict different behaviours for the thermal stratification inside the pool: in particular, the cold region below the THETIS outlet in RELAP5-3D reports a larger penetration capability with respect to the one predicted by CFD. In Fig. 9, instead, the temperature profile predicted inside the pool by the two codes is reported. As it can be noted, RELAP5-3D predicts a much lower mean temperature compared to the CFD results, with differences in the range of 15 °C, even in the assumed absence of heat transfer toward the environment. In this regard, it must be pointed out that the temperature profile used as boundary conditions for the CFD was obtained from the STH calculation: nevertheless, the temperatures predicted by CFD for the pool are much higher with respect to the one provided by RELAP5-3D. The observed discrepancies are mainly due to the larger heat transfer, in the range of 100 kW, predicted by CFD between the pool and the Fitting Volume: this difference did not occur in the previous CIRCE-HERO configuration chiefly owing to the different positioning of the SG outlet. In fact, since in the past configuration the steam generator outlet was located close to the loop inlet at the very bottom of the pool, the thermal stratification phenomenon occurred in the bottom region of the pool as well, leading to a hotter temperature distribution in the FV region. In that case, in fact, the smaller temperature differences between the fluid inside the Fitting Volume and the one in the nearby pool led to negligible heat transfer phenomena. With the new THETIS configuration, exhibiting instead an outlet section located well above the Fitting Volume, the thermal stratification occurs at a higher location, leading to a colder region in the pool region in

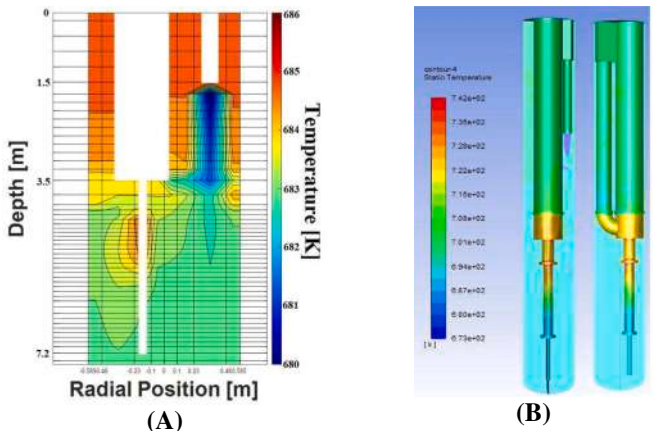

Fig. 8. Comparison between STH (A) and, CFD (B) results for the steady state condition.

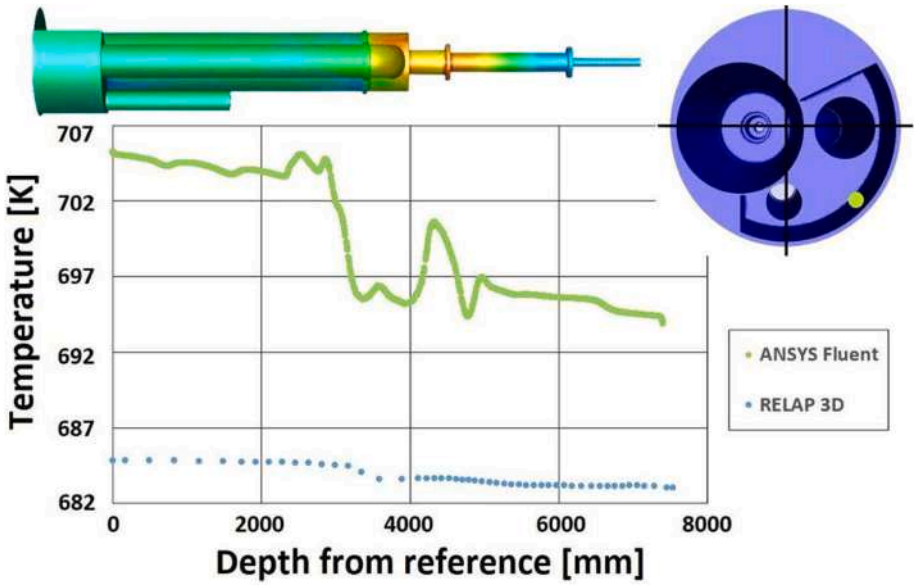

Fig. 9. Test reference results: temperature profile inside the pool.

correspondence of the Fitting Volume and to a consequent larger heat transfer. Unfortunately, while CFD predicts this occurrence, RELAP5 seems not able to sense the difference. Together with obvious differences related to the mesh size, allowing for a refined estimation adopting the CFD approach, it must be highlighted that the main cause of the predicted low heat transfer in RELAP5 is due to the differences in the considered modelling approach. While CFD adopts turbulence models allowing also for the estimation of local buoyancy phenomena, RELAP5 uses heat transfer correlations. In this regard, since the fluid in the pool flows very slowly, the predicted heat transfer coefficients are very small

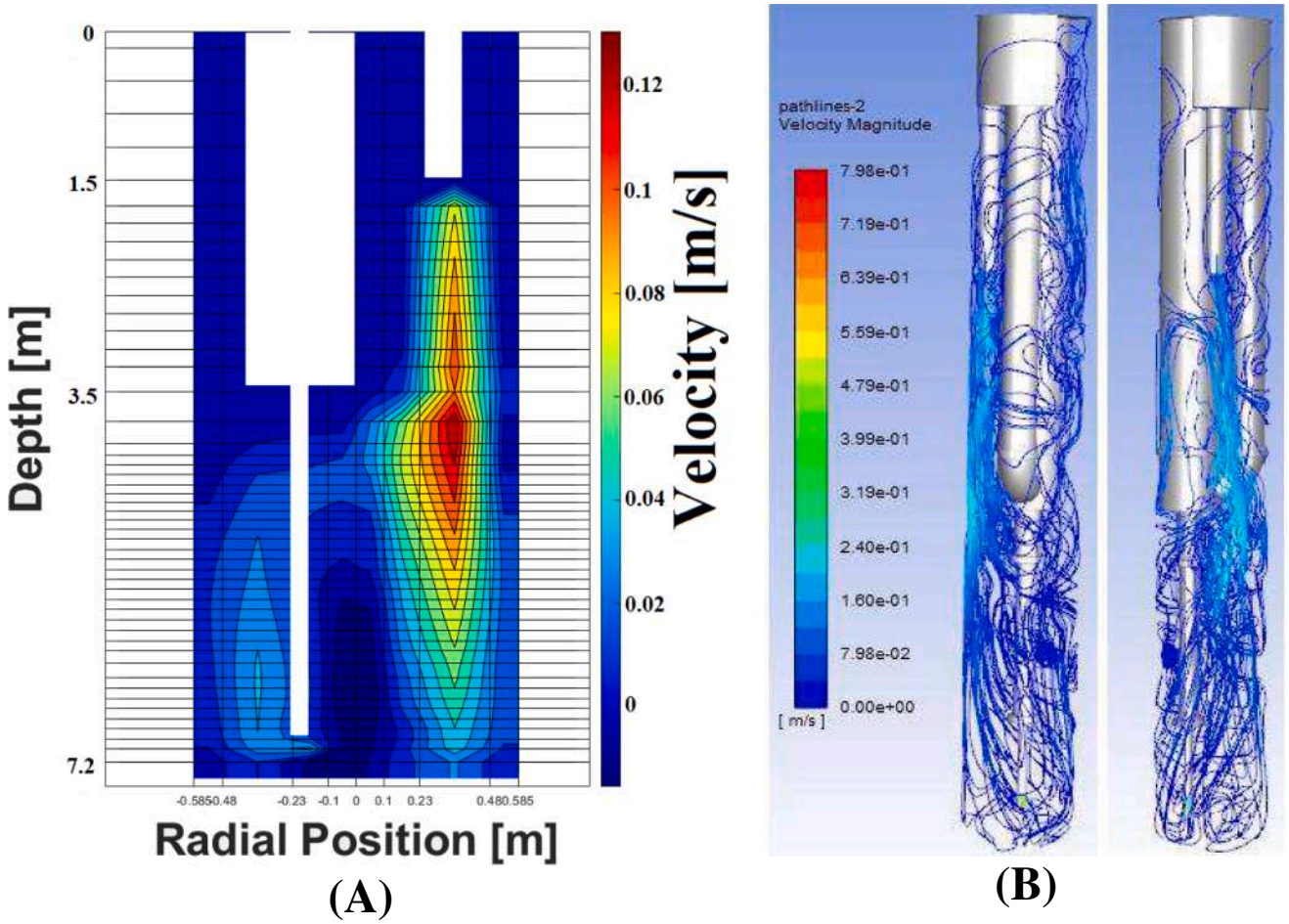

Fig. 10. Velocity field predicted by STH (A) and CFD (B) codes for the steady state conditions.

too, thus leading to the predicted smaller heat transfer across the FV walls. These results were considered relevant by the experimentalists: the predicted 100 kW were in fact considered excessive and undesired. Therefore, it was decided to improve the insulation of the FV in order to prevent the predicted large heat transfer phenomena. In addition, the predicted thermal stratification phenomenon also allowed for a preliminary estimation of the positioning of the thermocouples to be located inside the pool, suggesting the regions at which steeper variations are to be expected. As a final remark, at the present stage of the work, even if not matching, the obtained predictions may be considered sufficiently close. Indeed, the mean pool temperatures provided by the two codes differ by about 10 °C and the code-to-code comparison provides at least an idea of the phenomena which may occur inside the pool.

Looking at the velocity fields predicted by both the codes, a relevant difference can be highlighted. Fig. 10 shows that the velocities predicted by the STH code are usually smaller than the ones predicted by CFD, nevertheless a much larger penetration capability of the Steam Generator jet can be observed. These discrepancies are due to the obvious differences in the adopted mesh size: since larger volumes are considered in the RELAP5 application, smaller velocities, cutting the local peak values, are to be expected. For the penetration capabilities, instead, the differences are probably due to the lack in the STH code of shear forces that enhance the radial diffusion of the fluid. In the STH code, in fact, the LBE jet can easily reach the bottom part of the pool and goes directly towards the FPS inlet, as pointed out by the blue light branch at the bottom left of the Fig. 10a. All the mixing phenomena reported by CFD (see Fig. 10b) are completely absent in the RELAP5-3D prediction. This fact suggests that the STH code seems not able the well manage the present configuration of the CIRCE-pool. This limited capability is probably connected with the positioning of the steam generator outlet at the top of the pool. In the previous CIRCE-HERO facility, instead, with a steam generator outlet section located at the bottom of the pool, the CFD and STH prediction were in better agreement.

4.2. Postulated transient

The postulated transient starts from the reference steady-state condition reported in the previous section: the transient calculation performed adopting RELAP5-3D suggests that about 50000 s are required to reach these steady-state conditions. Once steady-state conditions were reached in the pool, the incidental scenario starts: feedwater flow rate is reduced and the pump is switched off in 10 s starting with one second of delay with respect to the power scram. The power supplied at the FPS is reduced following a postulated decay heat curve reported in Table 4. The simulation ran until the new steady-state condition was reached for the loop side. Once the MCP is switched off, the mass flow rate in the loop rapidly decreases. The mass flow passes from the 35.17 kg/s set during forced circulation to about 11 kg/s predicted for the new established natural circulation conditions. The temperature behaviour for the HX-outlet and for the FPS inlet and outlet sections is reported in Fig. 11a. As it can be noted, once the transient begins, the temperature at the FPS outlet drops following the FPS power decrease. It must be pointed out that, for the LBE temperature at the exit of the SG instead, a local peak is instead reported during the initial moments of the transient (see Fig. 11b). This phenomenon is due two main factors: the reduction in the feedwater mass flow rate (almost instantaneous) and the reduction in the power supplied at the FPS, which is experienced instead with a certain delay at the steam generator. In fact, the cold front, coming from the FPS takes about 120 s to reach the SG inlet: in the meantime, a temperature increase at the outlet section of the steam generator temperature is experienced since, owing to the almost instantaneous feedwater mass flow rate reduction, the steam generator is no more able to remove the nominal thermal load. During the first 700 s, no changes are experienced at the FPS inlet (Fig. 11b): the colder front in fact needs more time to reach this location and only at a later time (see Fig. 11a) the inlet temperature starts decreasing following the outlet trend. Sensitivity analyses on the temperature, power and mass flow rate transitions were performed as well. The results showed that too fast secondary water mass flow reductions may lead to undesired hot temperature values at the SG outlet sections. The performed analyses thus helped the experimentalists at obtaining a better understanding of the involved phenomena, suggesting potential risks for the facility during the postulated transitions and allowing for a better setting of the parameters of the test matrix.

Table 4
Decay heat curve.

Time (s)	Power %
0	100
1	25
2	22
3.5	19
5	17
10	15
22.5	10
30	9
50	8
60	7
90	6
180	6
240	5

Looking at the temperatures predicted by RELAP5-3D for the pool in Fig. 12a, it is clear the absence of axial conduction limits the modelling capabilities of this code. In fact, it can be noted that, due to buoyancies forces, the hot LBE is collected in the top part of the pool and at that location it is almost thermally insulated from the colder region in the bottom part. This way a tick region of hot fluid is predicted to occur at the top of the pool.

In the CFD results, instead, see Fig. 12b for reference, it can be noted that, owing to the refined nodalization and the different modelling approach, the predicted temperature distribution is more homogeneous and the hotter layer at the top of the pool is no more easily recognizable. In addition, a colder region can be spotted in the lowest part of the pool. The reasons of the presence of this region can be understood looking at the velocity fields predicted by the CFD and reported in Fig. 13b. Because of the reduced mass flow rate experienced at the SG outlet (from 35.17 to 11 kg/s) at the final steady-state, the flow jet exiting THETIS is weaker. Hence the mixing phenomena are suppressed and LBE is thus collected in the bottom region of the vessel. In fact, most of the fluid is mainly moved by natural convective motions that take place due to the heating from the FPS, while only a small portion of fluid reaches the bottom following a swirling motion. As consequence, the fluid in the lower part of the pool is almost stagnant and turns to be colder because of the heat exchange towards the environments through the external wall.

Fig. 13a points out, instead, the difficulties met by RELAP5-3D in dealing with large 3D environments. Even in this case, the LBE jet exiting THETIS easily reaches the bottom part of the pool, underling the wrong managing of viscus forces of the fluid itself. Being convinced that the CFD approach should be the most reliable for addressing the considered operating conditions, it thus seems that RELAP5-3D, while having shown success for other conditions, especially for thermal stratification in the CIRCE-HERO configuration (Stefanini, 2021), should not be instead considered suitable for the present CIRCE-THETIS application.

5. Conclusion

In the present paper, pre-test analyses for the new configuration of the CIRCE test section were performed. With respect to the old configuration, the new SG, named THETIS, presents a higher outlet section elevation and a more compact design. According to the performed analyses, this should enhance the mixing phenomena occurring inside the

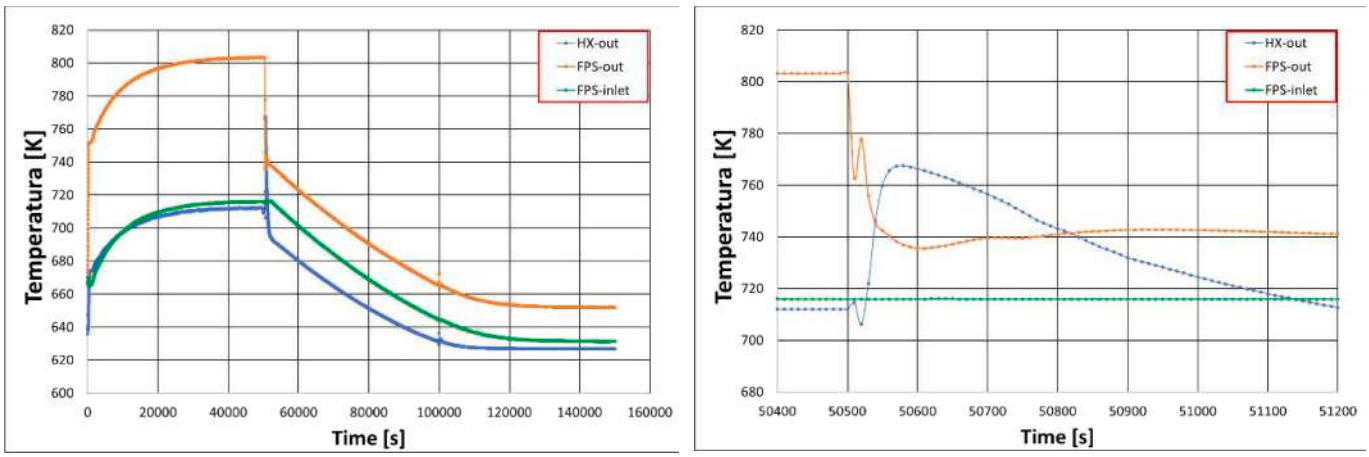

Fig. 11. Temperature trends predicted by RELAP5-3D (transient starts t = 50000 s): a) global trend, b) magnification of the behaviour during the initial moments of the transient.

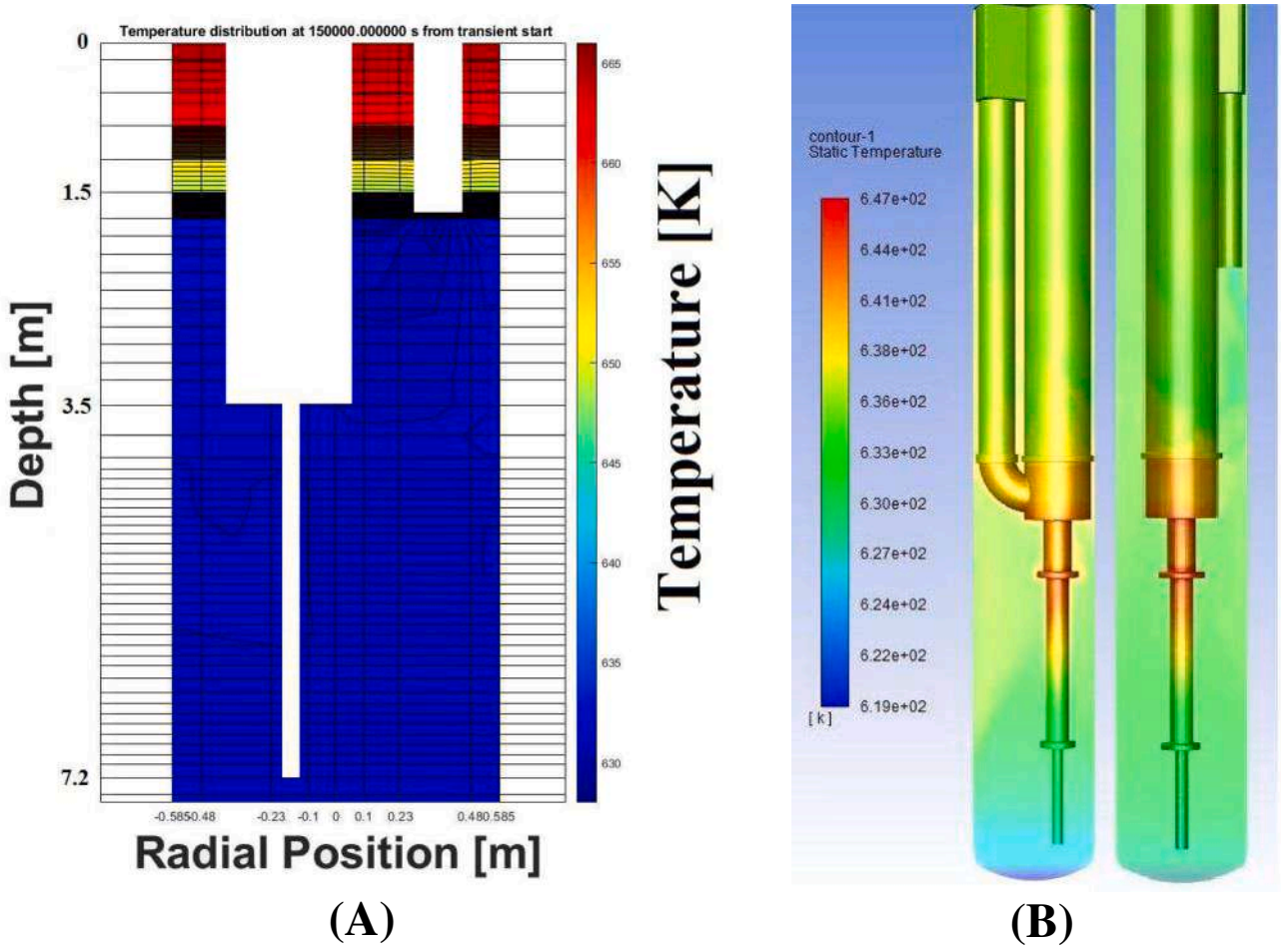

Fig. 12. Pool temperature distribution predicted by STH (A) and CFD (B) code (final steady state t = $1.5*10^6$s).

pool, weakening (but not preventing) the thermal stratifications reported by the old configuration. In fact, as pointed out in the considered reference steady state case, in this new test section layout a milder temperature transition from the bottom to the top part of the pool was predicted with respect to the old CIRCE-HERO configuration (Lorusso et al., 2018).

Concerning the comparison of the results provided by the two codes, it must be pointed out that RELAP5-3D seems not to be able to well manage the addressed large 3D environment. Looking at the velocity field predicted by the STH code, it seems that the cold jet of LBE exiting the SG is not sufficiently affected by the viscosity of the fluid itself and manages to reach the bottom of the pool with higher velocity. This high velocity may trigger a venturi effect near the heated region, that drags the heated LBE towards the FPS inlet; this way the heating up of the pool

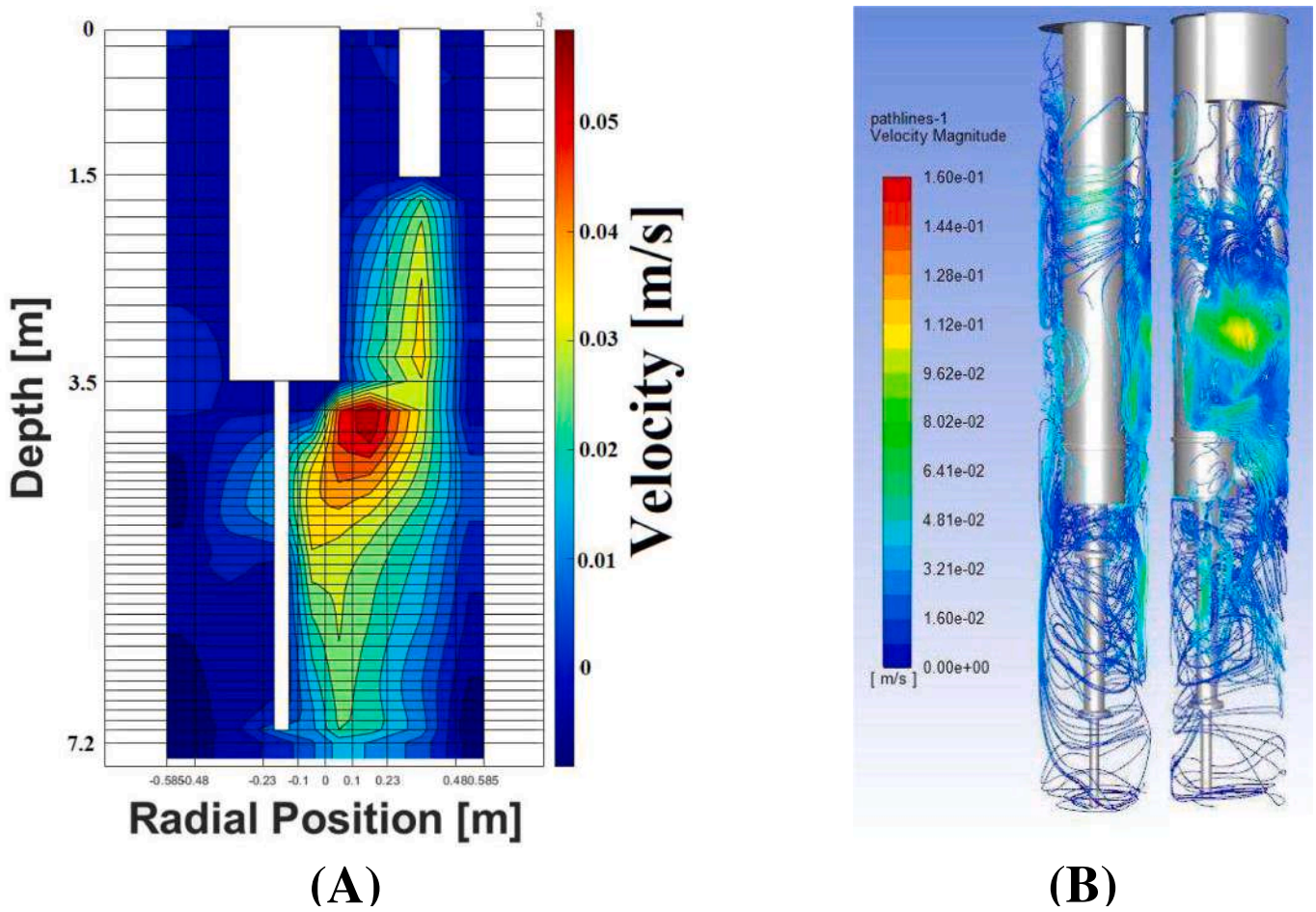

Fig. 13. Velocity field predicted by STH (A) and CFD (B) codes for the postulated transient (final steady state t = $1.5*10^6$s).

results less effective, leading to the low temperature distributions observed in the results section. In addition, potential gaps in the adopted heat transfer correlations for liquid metals may lead to the observed discrepancies with respect to the assumed more reliable CFD prediction.

The postulated transient was simulated only with RELAP5-3D, while CFD was considered for the final steady-state after the transient, adopting as boundary condition the values provided by RELAP5-3D. As in the previous case, RELAP5-3D seems not able to well manage the viscous stresses inside the fluid itself and, again, the LBE jet easily reaches the bottom part of the pool in contrast with the CFD prediction. In addition, lacking a model for pure axial conduction, in RELAP5-3D the hotter fluid is collected in the top part of the pool due to buoyancy forces and, once there, it remains almost thermally insulated by the colder fluid in the lower region, slowing down the cooling process of the pool.

Though the present work represents the first step in the pre-test analyses to be performed for the CIRCE-THETIS experimental campaign, the obtained results were already considered as relevant suggestions for the refinement of the test matrix and for the improvement of the experimental facility itself. The provided results will support the experimentalists in the positioning of the instrumentation and suggested the need for a better insulation of the FV in order to prevent large undesired heat transfer towards the pool. The analyses also suggest that, in this case, only CFD may provide suitable predictions of the pool environment, RELAP5-3D should thus be only considered for the internal loop. In this sense, in future works, together with a comparison of the numerical and experimental results, coupled STH/CFD calculations will be performed to better represent the interesting phenomena occurring inside the CIRCE-pool (CFD for the pool, STH for the loop and the secondary side) for both steady-state and transient conditions.

CRediT authorship contribution statement

Pietro Stefanini: Investigation, Formal analysis, Writing – original draft, Writing – review & editing. **Andrea Pucciarelli:** Writing – original draft, Writing – review & editing. **Nicola Forgione:** Supervision, Writing – original draft, Writing – review & editing. **Ivan Di Piazza:** Writing – original draft, Writing – review & editing. **Daniele Martelli:** Writing – original draft, Writing – review & editing.

Declaration of Competing Interest

The authors declare that they have no known competing financial interests or personal relationships that could have appeared to influence the work reported in this paper.

Data availability

Data will be made available on request.

Acknowledgements

This work has received funding from the European Union's Horizon 2020 Research and Innovation programme under grant agreement number 945077 in the frame of the PATRICIA project.

References

ANSYS, Inc., "ANSYS Fluent User's Guide, Release 19.2", August 2018.

Buzzi, F., Pucciarelli, A., Galleni, F., Tarantino, M., Forgione, N., 2020, "Analysis of the temperature distribution in the pin bundle of the CIRCE facility". Ann. Nucl. Energy, Volume 147, November 2020, 107717.

Buzzi, F., Pucciarelli, A., Galleni, F., Tarantino, M., Forgione, N., 2020. 2020, "Analysis of thermal stratification phenomena in the CIRCE-HERO facility". Ann. Nucl. Energy 141, 107320.

Di Piazza I., Lorusso P., Martelli D., Tarantino M., 2020. Experimental investigation of the transition between natural circulation modes in CIRCE. Kick-off meeting for PATRICIA, October 29th 2020 WP11-Task 11.11.

Galleni, F., Barone, G., Martelli, D., Pucciarelli, A., Lorusso, P., Tarantino, M., Forgione, N., 2020. Simulation of operational conditions of HX-HERO in the CIRCE facility with CFD/STH coupled codes. Nucl. Eng. Design 361, 110552.

Grishchenko, D., Jeltsov, M., Kööp, K., Karbojian, A., Villanueva, W., Kudinov, P., 2015. The TALL-3D facility design and commissioning test for validation of coupled STH and CFD codes. Nucl. Eng. Des. 290, 144–153.

IRSN, 2012, "Overview of Generation IV (GENIV) Reactor Designs, Safety and Radiological Protection Considerations.", IRSN Report 2012/158.

Lian, Q., Tian, W., Gao, X., Chen, R., Qiu, S., Su, G.H., 2020. Code improvement, separate-effect validation, and benchmark calculation for thermal-hydraulic analysis of helical coil once-through steam generator. Ann. Nucl. Energy 141, 107333.

Lorusso, P., Pesetti, A., Tarantino, M., Polazzi, G., Sermenghi, V., "CIRCE Experiment report" ENEA report for Project MYRTE, Ref. CI-I-R-353, 2018.

Lorusso P., Di Piazza I., Martelli D., Musolesi A., Tarantino M., 2021. Preliminary design of THETIS test section for the CIRCE facility. Enea report for MYRTE, Ref CI-I-R353.

Moscardini, M., Galleni, F., Pucciarelli, A., Martelli, D., Forgione, N., 2020. Numerical analysis of the CIRCE-HERO PLOFA scenarios. Appl. Sci. 2020 (10), 7358. https://doi.org/10.3390/app10207358.

MYRTE Project, 2015 MYRTE Project (No. Grant Agreement N. 662186), 2015. EURATOM H2020.

NUCLEAR ENERGY AGENCY, Handbook on Lead-bismuth Eutectic Alloy and Lead Properties, Materials Compatibility, Thermal hydraulics and Technologies, NEA No. 7268 © OECD 2015.

PATRICIA, https://patricia-h2020.eu/.

Pesetti, A., Forgione, N., Narcisi, V., Lorusso, P., Giannetti, F., Tarantino, M., 2018, "ENEA CIRCE-HERO test facility: geometry and instrumentation description", ENEA report for Project H2020 SESAME WP5.2, Ref CI-I-R-343.

Pucciarelli, A., Forgione, N., Martelli, D., Dovizio, D., Zwijsen, K., Moreau, V., Lampis, S., NFRP-09-2015. CIRCE Post-test CFD calculation report, Report D3.4 of the MYRTE project, Grant Agreement number: 662186 -. Activity 2019.

Pucciarelli, A., Galleni, F., Moscardini, M., Martelli, D., Forgione, N., 2020. STH/CFD Coupled simulation of the Protected Loss of Flow Accident in the CIRCE-HERO Facility. Appl. Sci. 10, 7032. https://doi.org/10.3390/app10207032.

Pucciarelli, A., Galleni, F., Moscardini, M., Martelli, D., N., December 2020. Forgione "STH/CFD coupled calculations of postulated transients from mixed to natural circulation conditions in the NACIE-UP facility". Nucl. Eng. Des. 370 (15) https://doi.org/10.1016/j.nucengdes.2020.110913.

Pucciarelli, A., Toti, A., Castelliti, D., Belloni, F., Van Tichelen, K., Moscardini, M., Galleni, F., Forgione, N., 2021. Coupled system thermal Hydraulics/CFD models: General guidelines and applications to heavy liquid metals. Ann. Nucl. Energy 153, 107990.

RELAP5-3D Code Manual, 2018, "RELAP5-3D code manual Volume I: Code structure, System models and solution methods". INL/MIS-1-36723 2018.

SESAME https://sesame-h2020.eu/.

Stefanini, P., 2021. Thermal Hydraulic Investigation of the CIRCE-THETIS Facility by the use of STH and CFD Codes, MSc Thesis in Nuclear Engineering. University of Pisa, Italy. DICI,.

Stefanini, P., Galleni, F., Di Piazza, I., Pucciarelli, A., 2023. Liquid-Metal Thermal-Hydraulic Numerical Analyses in Support of the Upcoming CIRCE-THETIS Experimental Campaign. Nucl. Technol. https://doi.org/10.1080/00295450.2023.2189892.

Stefanini, P., Pucciarelli, A., Forgione, N., "Analysis of the thermal stratification phenomena in the CIRCE pool by means of STH and CFD codes: state of the art and perspectives for future applications", Proceedings of NURETH-19, Mol, March 6 – 11, 2022.

K. van Tichelen, F. Mirelli, "Experimental investigation of steady state flow in the LBE-cooled scaled pool facility E-SCAPE", Proceedings of the 17th International Topical Meeting on Nuclear Reactor Thermal Hydraulics, Xi'an (China), September 3-8 (2017).

Xu, Z., Liu, M., Xiao, Y., Gu, H., 2021. Development of a RELAP5 model for the thermo-hydraulics characteristics simulation of the helically coiled tubes. Ann. Nucl. Energy 153, 108032.

Zwijsen, K., Dovizio, D., Moreau, V., Roelefs, F., 2019. CFD modelling of the CIRCE facility. Nucl. Eng. Design 353 (2019), 110277.